Published in final edited form as:
Circulation. 2005 September 6; 112(10): 1384–1391. doi:10.1161/CIRCULATIONAHA.105.543306.

Subunit Interaction Determines I_{Ks} Participation in Cardiac Repolarization and Repolarization Reserve

Jonathan Silva, MS and **Yoram Rudy, PhD**
From the Cardiac Bioelectricity and Arrhythmia Center, Washington University in St Louis, St Louis, Mo.

Abstract

Background—The role of I_{Ks}, the slow delayed rectifier K^+ current, in cardiac ventricular repolarization has been a subject of debate.

Methods and Results—We develop a detailed Markov model of I_{Ks} and its α-subunit KCNQ1 and examine their kinetic properties during the cardiac ventricular action potential at different rates. We observe that interaction between KCNQ1 and KCNE1 (the β-subunit) confers kinetic properties on I_{Ks} that make it suitable for participation in action potential repolarization and its adaptation to rate changes; in particular, the channel develops an available reserve of closed states near the open state that can open rapidly on demand.

Conclusions—Because of its ability to form an available reserve, I_{Ks} can function as a repolarization reserve when I_{Kr}, the rapid delayed rectifier, is reduced by disease or drug and can prevent excessive action potential prolongation and development of arrhythmogenic early afterdepolarizations.

Keywords

action potentials; electrophysiology; ion channels

Mutations to the cardiac potassium channel gene KCNQ1 (KvLQT1) have been linked to the long QT syndrome LQT1, which predisposes patients to arrhythmia during exercise and emotional stress, conditions that involve high levels of β-adrenergic stimulation. KCNQ1 is a 6-transmembrane domain protein that can form functional homomeric potassium channels and can also coassemble with the single transmembrane domain protein KCNE1 (MinK).[1] Together these gene products reconstitute the I_{Ks} channel. Mutations to KCNE1 have also been linked to LQT (LQT5).[2] In addition, transmural heterogeneity of I_{Ks} expression in ventricular myocardium gives rise to mid-myocardial cells (M cells) with a longer action potential (AP) duration (APD) and greater APD rate adaptation than epicardial or endocardial cells in many species.[3] I_{Ks} is also augmented by β-adrenergic stimulation,[4] suggesting its important role in mediating cardiac electrophysiological response.

These findings suggest that I_{Ks} is important for AP repolarization and APD adaptation to changes in rate, as demonstrated in guinea pig.[5–7] However, I_{Ks} density has been reported to be much lower in larger mammals, specifically in canine and human ventricle.[8] In canine myocytes, L-type calcium current, an inward depolarizing current, has been shown to mediate APD rate adaptation under control conditions without β-adrenergic effects.[7] However, AP repolarization requires a sufficient outward repolarizing current during phases

Correspondence to Yoram Rudy, PhD, Campus Box 1097, Whitaker Hall, Room 290, Washington University in St Louis, One Brookings Dr, St Louis, MO 63130-4899. E-mail rudy@wustl.edu.

2 and 3 of the AP. Such current is carried by I_{Kr} (the rapid delayed rectifier) and I_{Ks}, with I_{Kr} playing a primary role in large mammals under normal physiological conditions and in the absence of β-adrenergic stimulation. Because phases 2 and 3 depend on a delicate balance between inward and outward currents, one cannot rule out a priori an important role for I_{Ks}. Moreover, the arrhythmic consequences of LQT1 and LQT5[2] mutations, the existence of only 2 repolarizing currents (I_{Kr} and I_{Ks}) that constitute the delayed rectifier, and incorporation of the β-adrenergic signaling molecules into the I_{Ks} channel complex[4] strongly suggest an important role for I_{Ks} in human heart electrophysiology under various conditions. It has been hypothesized that in large mammals I_{Ks} constitutes a "repolarization reserve" (RR) that compensates for reductions in other repolarizing currents, in particular I_{Kr}, caused by mutations (hereditary LQT2) or drugs (acquired LQT syndrome).[9,10] There is growing consensus that in the absence of RR, certain drugs such as sotalol (antiarrhythmic), erythromycin (anti-infective), chlorpromazine (antipsychotic), and methadone can trigger a life-threatening arrhythmia.[9] The possibility of I_{Ks} generating this reserve and the dependence of I_{Ks} participation on its kinetics remain to be elucidated.

In the present study we examine the hypothesis that I_{Ks} can participate in AP repolarization because of kinetic properties conferred by interaction between its KCNQ1 and KCNE1 subunits. We present detailed, experimentally based Markov models of KCNQ1 and I_{Ks} and examine their kinetic behavior during the AP at slow and fast rates. By comparing KCNQ1 behavior with I_{Ks}, we isolate the effect of the modulatory KCNE1 subunit on the AP. Results show that because of its kinetic properties, I_{Ks} can create an available reserve (AR) of channels at fast rates that can open and generate a larger repolarizing current. In the presence of I_{Kr} block, this AR prevents excessive APD prolongation and the formation of arrhythmogenic early afterdepolarizations (EADs). Such properties are not present in homomeric KCNQ1 channels and therefore require interaction with KCNE1. The AR concept relates to reserve within a single channel, thereby extending the RR concept that involves compensation for one repolarizing current by another.

Methods

Markov models of KCNQ1 and I_{Ks} are derived from experimental data and published K^+ channel models.[11,12] Koren et al[11] described the K^+ delayed rectifier RCK1 with a Markov model of 4 independent voltage sensor transitions and 1 cooperative voltage-independent transition before the open state. Zagotta et al[12] expanded this model to study Shaker K^+ channels by assuming that each voltage sensor undergoes 2 conformational changes before channel opening and successfully reproduced delayed activation (sigmoidal activation). A delay of several milliseconds has also been observed for KCNQ1[13] and I_{Ks} activation,[14] suggesting that at least 2 voltage sensor transitions occur before channel opening. Experiments (J. Cui, PhD, personal communication, November 2004) also suggest a voltage-independent transition immediately before the first I_{Ks} open state, as proposed by Koren et al[11] for RCK1.

The Markov schemes we developed for KCNQ1 and I_{Ks} are shown in Figure 1A and 1B. Two closed-state zones are shown; green represents states in which at least 1 voltage sensor must still make a first transition, and blue represents states in which only faster second transitions are necessary for opening. Model derivation is described in the online-only Data Supplement. Criteria for fitting parameters are described below.

The KCNQ1 model is based on frog oocyte recordings[13] (Figure 2). Simulated activation to various potentials (Figure 2A), inactivation measured by a triple-pulse protocol (Figure 2C), and dependence of deactivation time constant on prepulse duration (Figure 2E) were included in the fitting procedure (details are in the online-only Data Supplement). The

reversal potential was −90 mV and temperature 23°C, as dictated by experimental conditions. (Sufficient KCNQ1 data are not available at 37°C). Model comparisons with experimental data are shown in Figure 2B, 2D, and 2F.

Lu et al[15] have recorded E-4031 insensitive current (I_{Ks}) in guinea pig ventricular myocytes at 37°C for $[K^+]_o$=5.4 mmol/L and $[Na^+]_o$=143 mmol/L (Figure 3A). Data were digitized from the published experimental figure, and ion concentrations were set as reported. Channels were assumed to be closed at −50 mV on the basis of the current-voltage relationship that shows no activation below −10 mV (Figure 3B). Therefore, instantaneous current (possibly due to leakage) was subtracted. Current tracings were normalized according to the current-voltage relationship curve so that the steady state value for each tracing would match the experimental average. Deactivation at −50 mV was fit directly to published data.[15] Rate of deactivation at resting V_m and current accumulation at fast pacing rates were simulated with I_{Ks} inserted in the whole-cell model (see below); comparison with experimental data[15] is shown in Figure 3B. Additionally, mean current increase at fast rates and dynamic conductance (corresponding to APs and I_{Ks} simulated in Figure 4) were compared with recordings from AP clamp[16] (Figure 5). A previously developed formulation of the reversal potential that accounts for sodium conductance through I_{Ks} channels was used (ratio of Na^+:K^+ permeability of 0.01833).[6]

Human I_{Ks} activation kinetics (Figure 3C) were fit to data from Kupershmidt et al,[17] who recorded expressed human I_{Ks} in HEK cells at 37°C. $[Na^+]_o$ was 145 mmol/L, and $[K^+]_o$ was 4 mmol/L. Expressed currents were fit because they display activation kinetics more clearly than currents recorded from native cells while still displaying activation at ≈−10 mV and a delay before slow activation, as in native cells.[8] Deactivation was constrained by time constants measured in human ventricular myocytes at 37°C for $[Na^+]_o$=144 mmol/L and $[K^+]_o$=4 mmol/L to ensure that open-state accumulation was not overestimated.[8] Reversal potential was calculated as for guinea pig I_{Ks}. Comparisons with experimental data are shown in Figure 3D.

Markov models for I_{Na}, I_{Kr} (updated version), and I_{Ks} were inserted in the Luo-Rudy (LRd) model of the guinea pig ventricular cell. AP simulation conditions are discussed in the online-only Data Supplement.

Results

KCNQ1 Model Validation and Current Properties

The KCNQ1 model (Figure 1A) was optimized to reproduce experimental protocols designed to isolate the essential channel features.[13] Sigmoidal activation is reproduced with multiple closed-state transitions before opening. This allows for minimal initial current followed by a steep rise after ≈3 ms, as observed experimentally[13] (Figure 2A). Two time constants of activation (fast followed by slow) are evident, with a slow rise in current observed even at 2-second depolarization, the last time point for which the current-voltage relationship is experimentally measured (Figure 2A, 2B).

Next, the triple-pulse protocol (Figure 2C, 2D), which measures channel inactivation at different potentials, is simulated. A short hyperpolarizing pulse to −130 mV allows most channels to recover from inactivation while preventing significant deactivation (Figure 2C). In the model, 5 open states allow channels to occupy open states far from the closed state (O_4 and O_5, Figure 2C), which delays deactivation during the hyperpolarizing pulse. However, transitions toward the closed state are rapid enough to reproduce the measured time constant of deactivation at −70 mV (Figure 2A; simulated τ_{deact}=377 ms, measured τ_{deact} 348 ms). Peak current and time constant of inactivation during the following (third)

pulse are consistent with experimental results[13] (Figure 2D), demonstrating rapid and voltage-dependent inactivation.

Finally, the dependence of deactivation time constant and relative inactivation (defined in the online-only Data Supplement) on pulse duration are simulated. KCNQ1 deactivation rate varies with pulse duration. As channels enter open states that are farther from the closed states, the rate of entry back into the closed states (τ_{deact}) is slowed (Figure 2F). τ_{deact} is greater than estimated experimentally from the dependence of deactivation on pulse duration (Figure 2E inset). However, a different experimental protocol (voltage dependence of deactivation) in the same study[13] estimates τ_{deact} close to the model-determined value at −60 mV (502±27 ms for experiment; 594 ms for model) with the same protocol. The different τ_{deact} from the 2 experimental protocols may be explained by the need to compensate for the inactivation hook in the pulse-duration protocol (Figure 2E inset) when fitting an exponential, a procedure that can have a major effect on the estimate of τ_{deact}. In the model such correction is not necessary because deactivation is measured directly as the decay of occupancy in the open and inactivated states.

In contrast to rapid inactivation during the third pulse (above), a single depolarizing pulse from −80 mV to 20 mV results in slow onset of inactivation (>200 ms pulse duration needed to elicit hook in tail current; Figure 2E) because of multiple transitions through open states. These transitions also govern relative inactivation (protocol not included in optimization), which shows an experimentally observed 75-ms delay[13] (Figure 2F).

I_{Ks} Model Validation and Current Properties

The I_{Ks} model resembles the KCNQ1 model closely, with the number of open-state transitions truncated and inactivation removed (Figure 1). Significant differences are introduced by changes in the transition rates. For example, increased KCNE1 mRNA in frog oocytes results in greater delay before activation.[14] This subunit effect is simulated by decreasing the transition rate from the first (resting) voltage sensor position (α) in the heteromeric guinea pig I_{Ks} channel to half the homomeric channel rate, confining more channels to zone 2 (Figure 3A, 3C insets). Once channels transition out of this zone, they activate rapidly. However, some channels remain in zone 2, causing a slow rise in current that continues even after several seconds (Figure 3A).

The first voltage sensor position is more stable for human I_{Ks} than KCNQ1 (C_1 occupancy is ≈9 times greater at −80 mV), resulting in slower activation and a continuous current increase even after a 5-second pulse to 60 mV. Once channels transition into O_1, they rapidly enter O_2 (at 40 mV, the rate into O_2 is 6.6 times faster than C_{15} to O_1). The presence of 2 open states allows for simultaneous reproduction of fast activation, steady state current-voltage relationship, and slow deactivation by facilitating slow deactivation without requiring slow activation to reproduce the steady state current.

I_{Ks} Role in Rate Adaptation of APD

Simulated whole-cell APs computed with the guinea pig I_{Ks} Markov model are shown at fast and slow pacing rates (Figure 4A). At the fast rate, peak I_{Ks} increases moderately compared with the slow rate (Figure 4B); however, the more rapid rise of I_{Ks} at the fast rate leads to greater repolarizing current earlier during the AP. This earlier I_{Ks} rise causes a 19.7% increase in mean I_{Ks} during the AP, from 1.27 μA/μF at cycle length (CL)= 1000 ms to 1.52 μA/μF at CL=250 ms. This is a conservative value compared with AP clamp experiments that measured a 28% increase at these rates.[16] The I_{Ks} increase during the AP accelerates repolarization to cause APD shortening at fast rates (adaptation).

I_{Ks} mediation of adaptation is a result of its closed-state transitions rather than its open-state accumulation. Figure 4C and 4D show total occupancy in zone 2 (green), zone 1 (blue), and the open states O_1 and O_2 (red) (Figure 1). During slow pacing (Figure 4C), most I_{Ks} channels reside in zone 2 before AP depolarization and must make a slow transition into zone 1 before opening. In contrast, at fast rates (Figure 4D) channels accumulate in zone 1 between APs, allowing I_{Ks} to activate rapidly via the second transition. There is not sufficient time between beats for the channels to transition back to zone 2 before the next AP, as at slow rates. Although there is some open-state accumulation due to slow deactivation, its effect on the current is opposed by the lower driving force resulting from a lower peak membrane potential at fast rates. Consequently, the primary mechanism for adaptation is the accumulation of closed states in zone 1, where a fast transition to the open states generates a rapid I_{Ks} rise during phase 1. Thus, at fast rates an AR is built ready to open very rapidly on demand. The overall low probability of channels residing in open states at slow and fast rates (Figure 4C, 4D) indicates that many channels are closed during the AP, creating a large I_{Ks} reserve.

AP clamp experiments have measured I_{Ks} conductance (g_{Ks}) during the AP at fast and slow rates, showing that open-state accumulation is minimal (Figure 5, bottom panel, arrows). Rather, I_{Ks} activates more rapidly at a fast rate than at a slow rate, as also observed in our simulations (Figure 5, top panel). The faster activation at fast pacing in experiments can be explained by the accumulation in closed states near to the open state that are readily available to open at the fast rate, as simulated by the model (Figure 4). Thus, the experiments support the concept of AR as a mechanism for I_{Ks} participation in repolarization and its dependence on rate.

Human I_{Ks} activates more slowly than guinea pig I_{Ks} and deactivates more rapidly (Figure 3C; compare with Figure 3A). The guinea pig cell provides a natural model for testing I_{Ks} in an environment in which I_{Kr} plays only a secondary role in repolarization. To evaluate the capability of human I_{Ks} to serve as a RR and to compensate for reduced I_{Kr}, we inserted a model of human I_{Ks} in the guinea pig LRd model (Figure 6). As can be seen in Figure 6F (solid line), with increased maximum conductance, human I_{Ks} can generate APD adaptation (g_{Ks} ≈4 times greater than guinea pig to obtain 200 ms APD). In contrast, when homomeric KCNQ1 channels are inserted, there is less APD adaptation at fast rates (Figure 6F, dashed line). This attenuation of APD adaptation is surprising because the deactivation kinetics of KCNQ1 are slower than human I_{Ks}, allowing for open-state accumulation (Figure 6D). However, I_{Ks} channels accumulate in zone 1 (Figure 6E, black), which is composed of closed states that only require rapid transitions to open, allowing for rapid activation that leads to large current during the repolarization phase of the AP (Figure 6C, thin line). This large I_{Ks} current during repolarization proves more important for shortening APD than the instantaneous current generated by KCNQ1. As shown earlier (Figure 4), zone 1 accumulation rather than open-state accumulation underlies the increase of I_{Ks} at fast rates. Such AR closed-state accumulation in zone 1 does not occur in KCNQ1 channels (Figure 6E, gray). Instead, a large percentage of channels activate even at slow rates (open-state occupancy at CL=10 000 ms is 30% for KCNQ1 versus 7% for I_{Ks}), preventing an increase at fast rates.

I_{Ks} and KCNQ1 During I_{Kr} Block

Figure 7A shows mean I_{Ks} (black) compared with KCNQ1 current (gray) during the first and 40th APs at CL=500 ms. I_{Ks} increases ≈50% from the first to the 40th AP, whereas KCNQ1 remains almost the same over 40 paced beats (inset shows current tracings for the first 9 beats). When I_{Kr} is blocked, greater I_{Ks} increase is observed over 40 paced beats (relative to control conditions), whereas only a limited increase is noted for KCNQ1. The difference between I_{Ks} and KCNQ1 behavior in the presence of I_{Kr} block is due to the

nature of current accumulation. I_{Kr} block prolongs the AP plateau and elevates its potential, thus enhancing transitions toward the open states. KCNQ1 accumulation is mostly in the open state, which is at the expense of populating closed states that constitute the AR. Consequently, most channels open on every beat, allowing for only limited accumulation between beats. In contrast, I_{Ks} shows minimal open-state accumulation, and I_{Kr} block facilitates transitions into closed states that constitute the AR, allowing for greater I_{Ks} accumulation over many beats.

When a pause is simulated after 40 beats in the presence of I_{Kr} block (Figure 7B), the postpause AP with KCNQ1 develops an EAD as a consequence of insufficient KCNQ1 current late during the AP. In contrast, the AP with I_{Ks} repolarizes normally because of the superior ability of I_{Ks} to activate during phase 3 of a prolonged AP.

Discussion

We show that interaction of KCNQ1 with the β-subunit KCNE1 to form I_{Ks} alters kinetics so that an AR is created at fast pacing rates. In contrast to KCNQ1, which does not generate a significant AR, I_{Ks} causes greater APD adaptation and protects against EADs when I_{Kr} is reduced.

The AR concept can be examined experimentally. For example, a gapped double-pulse protocol with variation in the gap width could be used to characterize the AR in both guinea pig and human ventricular myocytes. In this protocol, a depolarizing pulse to 40 mV for 2 seconds would activate the channel. This step would then be followed by a repolarizing step of variable duration (from 10 ms to 1 second) to −80 mV so that the channel could partially deactivate. A second depolarizing pulse to 40 mV would be used to measure the rate of activation, providing a measure of the AR.

Our simulations also predict that I_{Ks} will increase more at fast rates when I_{Kr} is blocked (Figure 7), a manifestation of AR. This prediction could be experimentally tested by blocking I_{Kr} and measuring the increase in I_{Ks} during an AP clamp at slow and fast rates. Another protocol to test interaction between I_{Kr} and I_{Ks} would be to reduce I_{Ks} and measure the change in APD from control during pacing, and then to apply I_{Kr} reduction to control and block I_{Ks} to the same degree as in the previous protocol. Our simulations predict that the same I_{Ks} reduction will have a much greater effect on APD when I_{Kr} is also reduced.

At fast rates, the ability of guinea pig I_{Ks} to accumulate between APs allows it to participate in APD shortening. However, in human myocytes I_{Ks} deactivates rapidly, bringing into question its ability to accumulate and mediate APD adaptation. Our simulations show that open-state accumulation is not necessary for I_{Ks} to increase at fast rates. Because of the complex nature of potassium channel activation, channels can accumulate in closed states near the open states (zone 1) to form an AR that opens rapidly and generates large I_{Ks} current during AP repolarization. This effect is confirmed by AP clamp experiments[16] that show little accumulation in the open state but rapid activation at fast rates (Figure 5) that leads to greater I_{Ks} during the AP. In canine myocytes, I_{Ks} accumulation is also observed in the presence of β-agonist.[18] Here the mechanism of I_{Ks} accumulation is identical for both human and guinea pig I_{Ks}, indicating a common mechanism for I_{Ks} increase across species.

This novel mechanism of adaptation contrasts with the behavior of homomeric KCNQ1 channels that accumulate in the open states because of slow deactivation but show no significant AR. Consequently, the KCNQ1 AP does not adapt as much as the I_{Ks} AP (Figure 6). The fundamental difference between I_{Ks} and KCNQ1 channels is the degree of participation of the first voltage sensor transition in channel activation. Because of the stabilization of the voltage sensor first position by KCNE1, only a small fraction of I_{Ks}

channels activate at slow rates, creating a reserve of channels that can activate at fast rates to accelerate repolarization. In contrast, a large percentage of KCNQ1 channels activate even at slow rates, preventing buildup of such a reserve. As shown in Figure 6C, the initial jump (arrow) of I_{Ks} current that reflects open-state accumulation at fast rates is small and is followed by a steady increase to a peak of 3.4 μA/μF late during the AP. At this phase of the AP, I_{Ks} has a maximal effect on repolarization and APD. In contrast (Figure 6D), KCNQ1 current displays a large initial jump (arrow) due to large open-state accumulation but does not increase during the AP in the absence of an AR; its magnitude stays at ≈2 μA/μF and lacks the late peak that is important for repolarization. Thus, interaction with the KCNE1 subunit strongly influences the I_{Ks} profile during the AP; it augments AP shortening and is essential to normal I_{Ks} function and its participation in APD adaptation. Other differences between KCNQ1 and I_{Ks}, such as open-state behavior and flickery block, are discussed in the online-only Data Supplement.

As stated earlier in this report, I_{Ks} is not likely to participate in rate adaptation in large mammals under control conditions.[7] However, when I_{Kr} is reduced, I_{Ks} is the only remaining major repolarizing current. The guinea pig myocyte provides a natural electrophysiological environment in which I_{Kr} is reduced. Under these conditions, we show that human I_{Ks} can mediate rate adaptation when the maximum conductance of the current is increased (Figure 6). β-Agonists, which are present in the normal physiological environment even at basal heart rates, can readily confer such an increase in I_{Ks} conductance.

In the case of pathologically reduced I_{Kr} (by a mutation or a drug), outward currents carried by other channels (RR) can prevent excessive APD prolongation, EADs, and triggered activity. It is hypothesized that I_{Kr} reduction in conjunction with a compromised RR is a precursor to arrhythmia, especially after a pause.[9] To test the ability of I_{Ks} to participate in the RR, we compared I_{Ks} with KCNQ1 accumulation under control conditions and with I_{Kr} block. During pacing, I_{Ks} displays greater accumulation than KCNQ1 and increases further when I_{Kr} is reduced (Figure 7A). When the pause protocol is simulated with blocked I_{Kr}, increased I_{Ks} results in normal repolarization, whereas the postpause AP with KCNQ1 develops an EAD (Figure 7B). These simulations indicate that the ability of I_{Ks} to form an AR, which leads to accumulation at fast rates, makes it an ideal candidate to play a critical role in RR. The accepted RR concept involves compensation for one repolarizing current by another. This study demonstrates the existence of a reserve (AR) within a single channel (I_{Ks}), thereby extending the RR concept to include single-current reserve.

We describe I_{Ks} with 2 transitions, a slow transition (to zone 1) followed by a fast transition (to open), which implies that a 2-closed-state model (rather than 15 states) representing lumped voltage sensor transitions could adequately describe I_{Ks} activation. However, this model would not reproduce the experimentally observed delay before activation,[14,19] which has important consequences during the AP. To reproduce these kinetics, a semi-Markov 2-closed-state model could be used that would introduce a memory property to the channel via time-dependent transition rates. Such models have been proposed[20] but introduce another level of complexity with the addition of memory. The present model was chosen because of its correlation to the tetrameric symmetry of K^+ channels and the simplicity of 4 transitions without memory that describe I_{Ks} activation. This detailed description of activation, in particular the delay before activation, is a channel feature that has not previously been incorporated into an I_{Ks} model.

Model parameters were determined with the use of nonlinear optimization. Although we incorporated a large set of experiments, there may be different parameters that also reproduce channel properties. Our conclusions depend on the participation of numerous closed states in I_{Ks} activation. The necessity of these states for generating a delay before

activation has been rigorously documented.[19] Thus, any model of this topology (Figure 1) that fits I_{Ks} activation, regardless of the parameter set, would generate an AR and cause more adaptation at fast rates (see online-only Data Supplement).

Not all data were obtained from native myocytes. For KCNQ1, we used frog oocyte experiments13 conducted at room temperature, in which transition rates differ from body temperature. Still, KCNQ1 activation in mammalian cells (37°C)[1] and in oocytes (25°C) is quite similar, with 2 time constants of activation and similar current-voltage relationships.

Future work should incorporate β-adrenergic modulation of I_{Ks} and study its effects on whole-cell electrophysiological function. To accomplish this, a β-adrenergic model that simulates its effects on many cellular processes is necessary; these processes include sarcoplasmic reticulum calcium handling, $I_{Ca,L}$, the transient outward Cl^- current ($I_{to,2}$), I_{Na}, I_{NaCa}, I_{Ks}, and I_{K1}. To date there have been attempts to create such a model,[21,22] but a sufficiently complete model that allows accurate study of AP dynamics in the context of β-adrenergic stimulation awaits development.

Supplementary Material

Refer to Web version on PubMed Central for supplementary material.

Acknowledgments

This work was supported by National Institutes of Health/National Heart, Lung, and Blood Institute grants R01-HL49054 and R37-HL33343 (Dr Rudy) and F31-HL68318 (Dr Silva). Dr Rudy is the Fred Saigh Distinguished Professor of Engineering. We thank J. Cui, T. Hund, G. Faber, K. Decker, and T. O'Hara for helpful discussions and M. Sanguinetti for KCNQ1 data.

References

1. Sanguinetti MC, Curran ME, Zou A, Shen J, Spector PS, Atkinson DL, Keating MT. Coassembly of K(V)LQT1 and minK (IsK) proteins to form cardiac I(Ks) potassium channel. Nature 1996;384:80–83. [PubMed: 8900283]
2. Splawski I, Tristani-Firouzi M, Lehmann MH, Sanguinetti MC, Keating MT. Mutations in the hminK gene cause long QT syndrome and suppress IKs function. Nat Genet 1997;17:338–340. [PubMed: 9354802]
3. Antzelevitch, C.; Dumaine, R. Electrical heterogeneity in the heart: physiological, pharmacological and clinical implications. In: Page, E.; Fozzard, H.; Solaro, J., editors. Handbook of Physiology, Section 2: The Cardiovascular System, Volume I: The Heart. New York, NY: Oxford University Press; 2002. p. 654-692.
4. Marx SO, Kurokawa J, Reiken S, Motoike H, D'Armiento J, Marks AR, Kass RS. Requirement of a macromolecular signaling complex for beta adrenergic receptor modulation of the KCNQ1-KCNE1 potassium channel. Science 2002;295:496–499. [PubMed: 11799244]
5. Sicouri S, Quist M, Antzelevitch C. Evidence for the presence of M cells in the guinea pig ventricle. J Cardiovasc Electrophysiol 1996;7:503–11. [PubMed: 8743756]
6. Viswanathan PC, Shaw RM, Rudy Y. Effects of IKr and IKs heterogeneity on action potential duration and its rate dependence: a simulation study. Circulation 1999;99:2466–2474. [PubMed: 10318671]
7. Hund TJ, Rudy Y. Rate dependence and regulation of action potential and calcium transient in a canine cardiac ventricular cell model. Circulation 2004;110:3168–3174. [PubMed: 15505083]
8. Virag L, Iost N, Opincariu M, Szolnoky J, Szecsi J, Bogats G, Szenohradszky P, Varro A, Papp JG. The slow component of the delayed rectifier potassium current in undiseased human ventricular myocytes. Cardiovasc Res 2001;49:790–797. [PubMed: 11230978]
9. Roden DM. Drug-induced prolongation of the QT interval. N Engl J Med 2004;350:1013–1022. [PubMed: 14999113]

10. Volders PG, Stengl M, van Opstal JM, Gerlach U, Spatjens RL, Beekman JD, Sipido KR, Vos MA. Probing the contribution of IKs to canine ventricular repolarization: key role for beta-adrenergic receptor stimulation. Circulation 2003;107:2753–2760. [PubMed: 12756150]
11. Koren G, Liman ER, Logothetis DE, Nadal-Ginard B, Hess P. Gating mechanism of a cloned potassium channel expressed in frog oocytes and mammalian cells. Neuron 1990;4:39–51. [PubMed: 2310574]
12. Zagotta WN, Hoshi T, Aldrich RW. Shaker potassium channel gating, III: evaluation of kinetic models for activation. J Gen Physiol 1994;103:321–362. [PubMed: 8189208]
13. Tristani-Firouzi M, Sanguinetti MC. Voltage-dependent inactivation of the human K+ channel KvLQT1 is eliminated by association with minimal K+ channel (minK) subunits. J Physiol 1998;510(pt 1):37–45. [PubMed: 9625865]
14. Cui J, Kline RP, Pennefather P, Cohen IS. Gating of IsK expressed in Xenopus oocytes depends on the amount of mRNA injected. J Gen Physiol 1994;104:87–105. [PubMed: 7964597]
15. Lu Z, Kamiya K, Opthof T, Yasui K, Kodama I. Density and kinetics of I(Kr) and I(Ks) in guinea pig and rabbit ventricular myocytes explain different efficacy of I(Ks) blockade at high heart rate in guinea pig and rabbit: implications for arrhythmogenesis in humans. Circulation 2001;104:951–956. [PubMed: 11514385]
16. Rocchetti M, Besana A, Gurrola GB, Possani LD, Zaza A. Rate dependency of delayed rectifier currents during the guinea-pig ventricular action potential. J Physiol 2001;534:721–732. [PubMed: 11483703]
17. Kupershmidt S, Yang IC, Sutherland M, Wells KS, Yang T, Yang P, Balser JR, Roden DM. Cardiac-enriched LIM domain protein fhl2 is required to generate I(Ks) in a heterologous system. Cardiovasc Res 2002;56:93–103. [PubMed: 12237170]
18. Stengl M, Volders PG, Thomsen MB, Spatjens RL, Sipido KR, Vos MA. Accumulation of slowly activating delayed rectifier potassium current (IKs) in canine ventricular myocytes. J Physiol 2003;551:777–786. [PubMed: 12819301]
19. Zagotta WN, Hoshi T, Dittman J, Aldrich RW. Shaker potassium channel gating, II: transitions in the activation pathway. J Gen Physiol 1994;103:279–319. [PubMed: 8189207]
20. Clay JR. A simple model of K+ channel activation in nerve membrane. J Theor Biol 1995;175:257–262. [PubMed: 7564400]
21. Zeng J, Rudy Y. Early afterdepolarizations in cardiac myocytes: mechanism and rate dependence. Biophys J 1995;68:949–964. [PubMed: 7538806]
22. Saucerman JJ, Brunton LL, Michailova AP, McCulloch AD. Modeling beta-adrenergic control of cardiac myocyte contractility in silico. J Biol Chem 2003;278:47997–48003. [PubMed: 12972422]

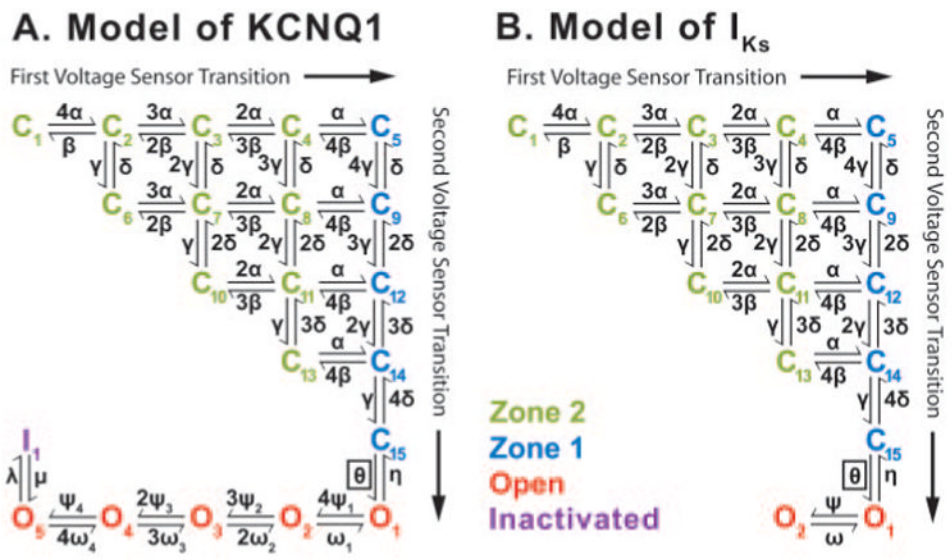

Figure 1.

KCNQ1 and I_{Ks} Markov models. A, Model of KCNQ1 contains 15 closed (C_1 to C_{15}) states to account for 2 transitions of each of the 4 voltage sensors before channel opening. Green closed states represent channels in zone 2 that have not completed the first transition for all 4 channel subunits. Blue closed states represent channels in zone 1 that have completed 4 first voltage sensor transitions. The boxed transition (θ) to the open state is voltage independent. There are 5 open states (O_1 to O_5, red) and an inactivation state (I, purple). B, Model of I_{Ks} contains 2 open states with no inactivation.

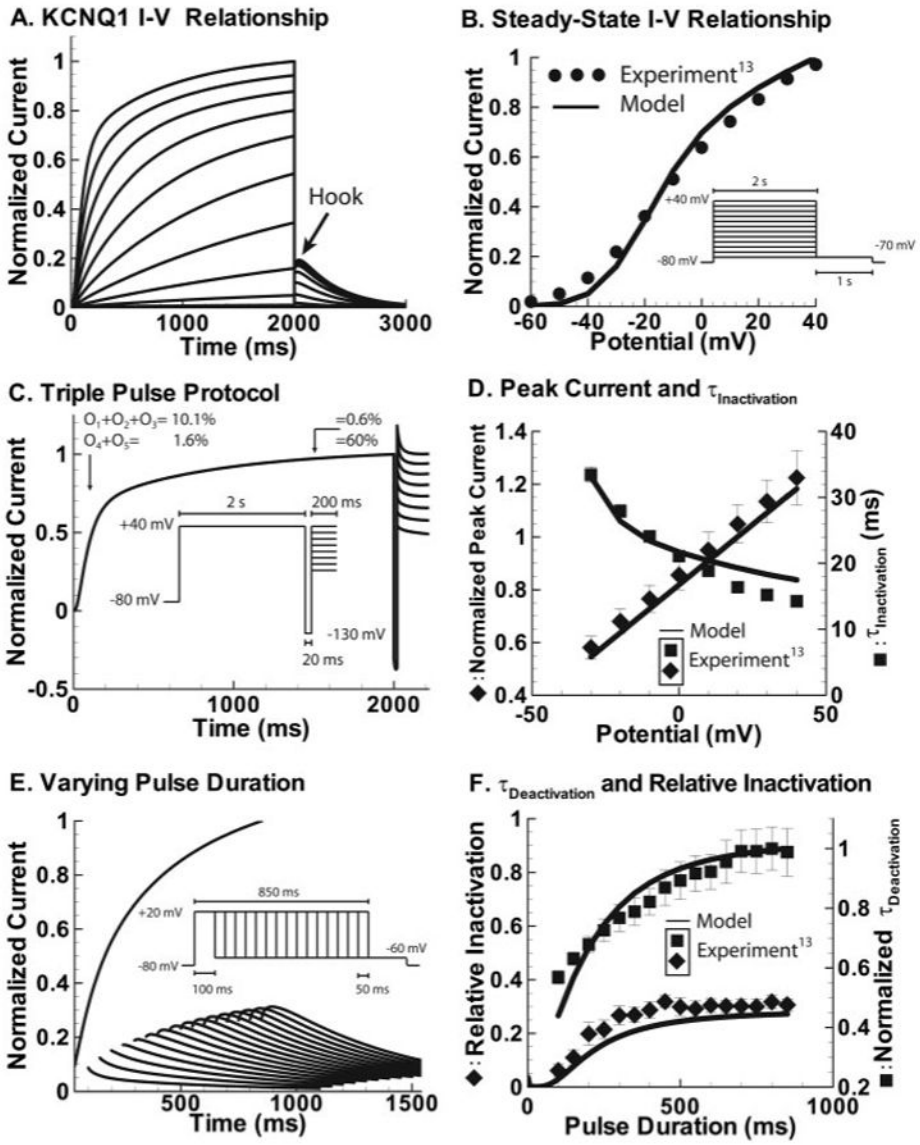

Figure 2.

KCNQ1. A, Simulated current resulting from steps from −80 mV to various potentials (−70 to 40 mV) followed by a step to −70 mV (protocol shown in B). After stepping down to −70 mV, a hook is observed in the tail current indicating presence of inactivation, as observed experimentally.[13] B, Simulated steady state current-voltage (I–V) curve (solid line) obtained from the protocol in A is compared with experiment (circles). C, Simulated current resulting from triple-pulse protocol (inset). Current resulting from the second depolarizing pulse shows no reactivation, indicating a delay before deactivation. The delay is due to accumulation in O_4 and O_5, as can be seen by the percentage (shown above tracing) of channels in these states late during the pulse. D, Simulated peak current for the second depolarizing pulse in C (solid line) normalized to the maximum current at 40 mV is compared with experiment (diamonds). Time constant of inactivation (from protocol in C) is also compared with experiment (squares). E, Simulated tail currents after various prepulse durations (protocol in inset). F, Relative inactivation and deactivation time constant with

varying pre-pulse duration from the protocol in E. Simulated time constant of deactivation is normalized to 739 ms; experimental time constants (squares) are normalized to 365 ms. Relative inactivation is also compared with experiment (diamonds). B, D, and F were adapted from reference [13] with permission from Blackwell Publishing.

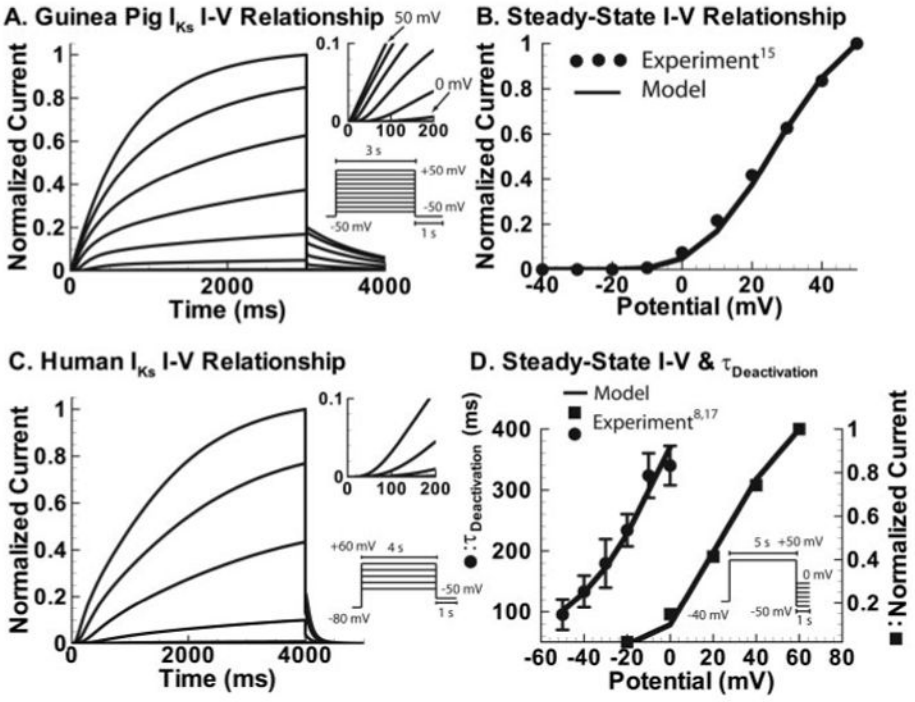

Figure 3.

Guinea pig and human I_{Ks}. A, Simulated guinea pig I_{Ks} current resulting from protocol in inset. A delay of several milliseconds is observed before depolarization at voltages <20 mV and is inversely proportional to voltage (inset enlarges the initial portion of the current tracings). Tail currents show no hook, indicating absence of inactivation, as in experiment. B, Simulated steady state guinea pig current-voltage (I–V) relationship from the protocol in A is compared with experiment (circles). Adapted from reference [15] with permission from Lippincott Williams and Wilkins. C, Human I_{Ks} current resulting from the protocol in inset. Activation is slower than guinea pig I_{Ks} with a longer (20 ms) delay, and tail currents deactivate faster, as observe experimentally. D, Simulated steady state I–V relationship for human I_{Ks} compared with experiment17 (squares, protocol in C) and time constant of deactivation compared with experiment[8] (circles, protocol in D inset). Adapted from references 8 and 17, copyright 2001 and 2002, with permission from The European Society of Cardiology.

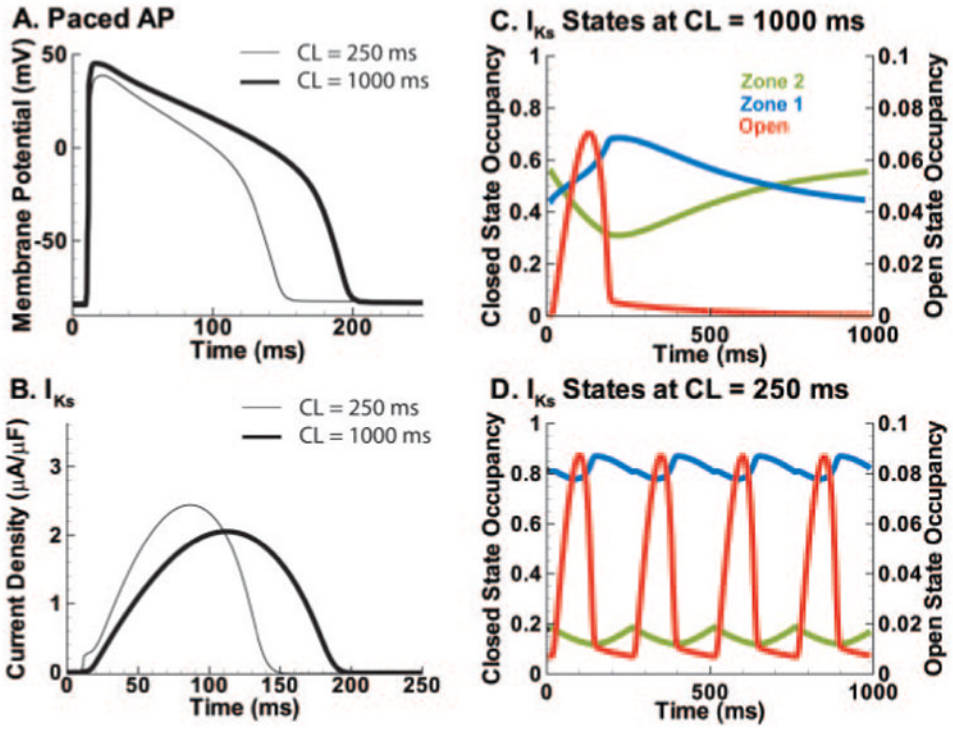

Figure 4.

I_{Ks} role in APD adaptation. A, Fortieth AP at CL=250 ms (thin line) and CL=1000 ms (thick line) under control conditions. B, Guinea pig I_{Ks} during the APs in A. C, State occupancy during the 40th AP at slow rate (1000 ms). Green shows occupancy in zone 2 (Figure 1). Blue shows occupancy in zone 1. Red shows open channel occupancy (O_1+O_2). At AP initiation, most channels reside in zone 2. D, Occupancies at fast rate (CL=250 ms); same format as C. At the AP initiation, most channels reside in zone 1. Accumulation in zone 1 facilitates channel opening and larger I_{Ks} during the AP (B), causing APD shortening (A). Buildup of zone 1 reserve underlies the participation of I_{Ks} in APD rate adaptation. Open-state accumulation is minimal.

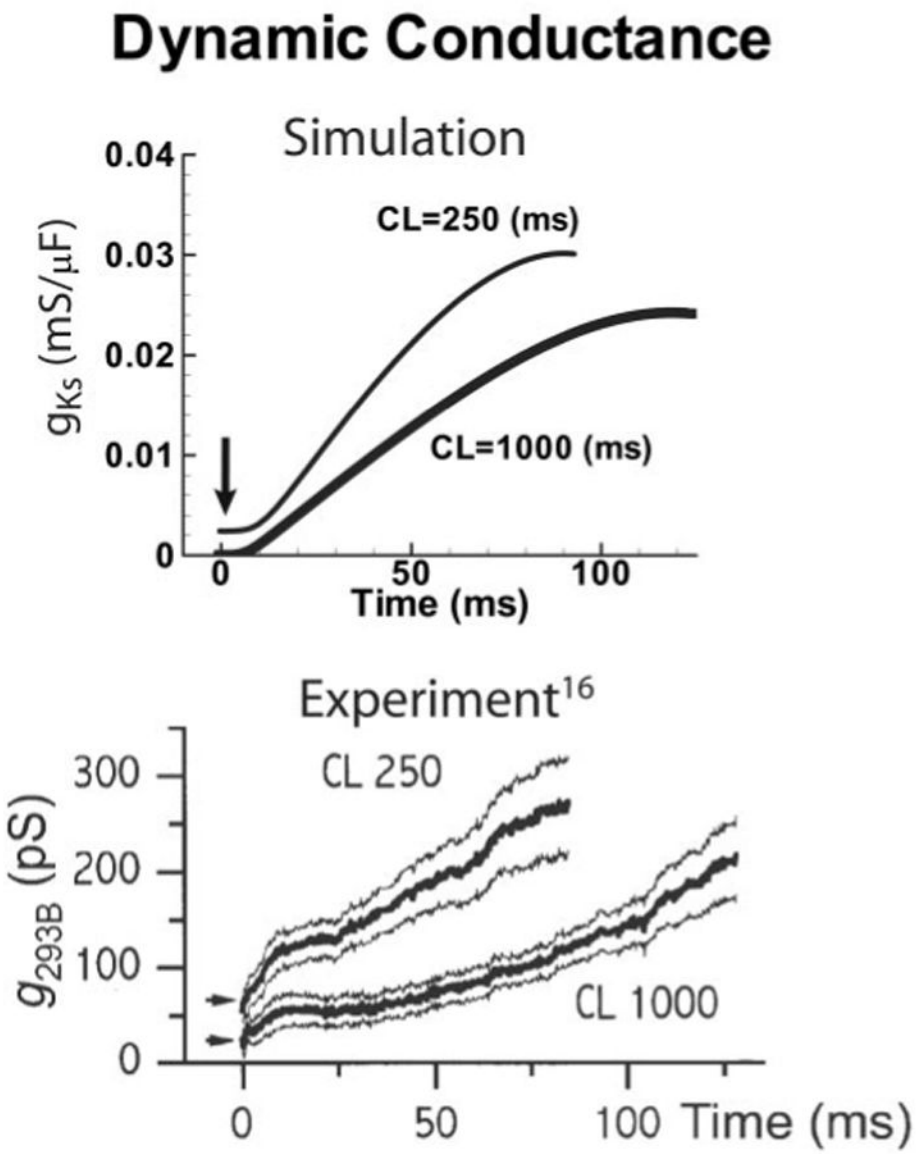

Figure 5.

Dynamic guinea pig I_{Ks} conductance during AP clamp. Bottom, Experimentally measured I_{Ks} conductance (Chromanol 293B–sensitive current, g_{293B}) at fast (CL=250 ms) and slow rates (CL=1000 ms) (thick and thin lines are mean and confidence limits, respectively). Arrows indicate open-state occupancy at AP outset. Reprinted from reference [16] with permission from Blackwell Publishing. Top, Simulation also shows little open-state accumulation (arrow) even at fast rates; instead, in both simulation and experiment an increase in I_{Ks} activation rate during fast pacing is responsible for greater I_{Ks} during the AP.

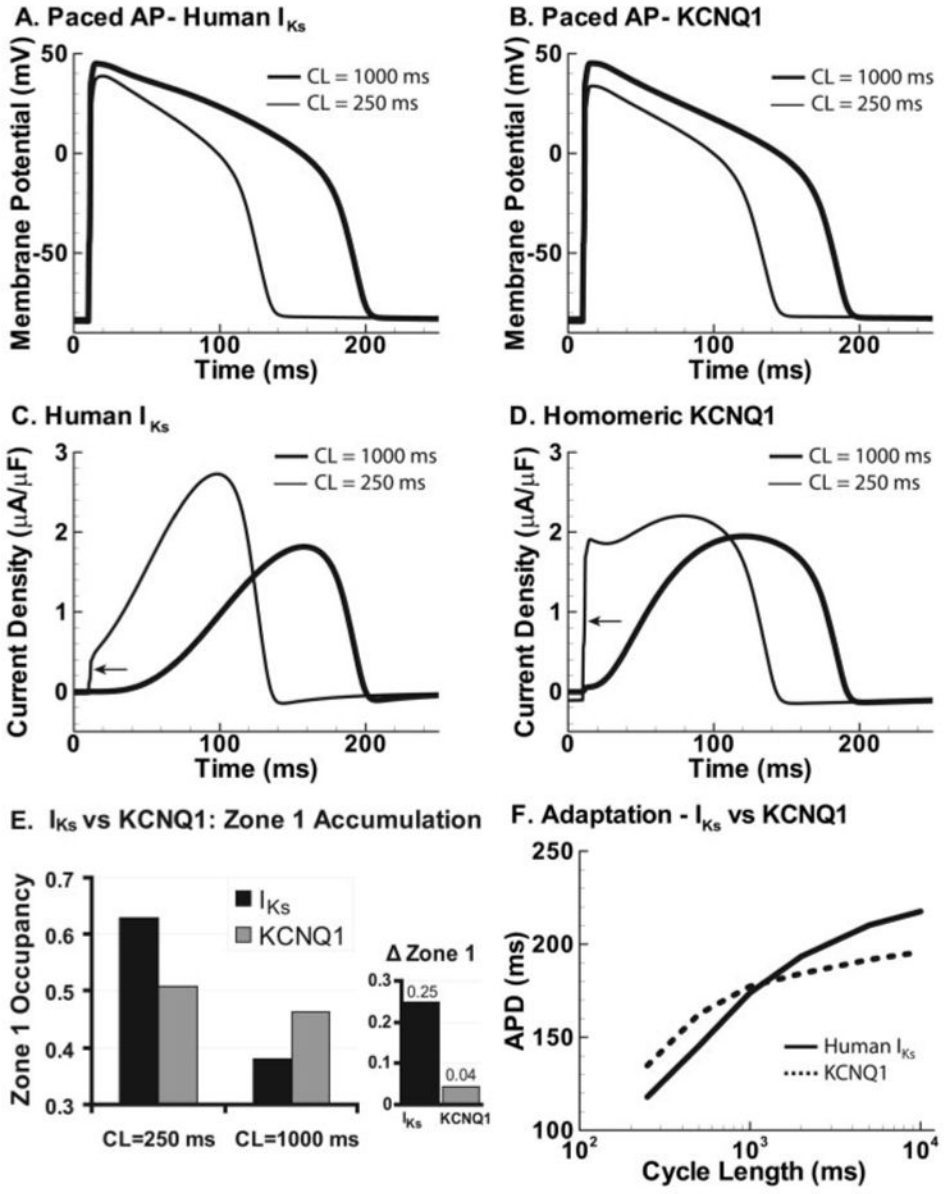

Figure 6.

Adaptation with human I_{Ks} vs human KCNQ1. A, Fortieth AP shown at CL=250 ms (thin line) and at 1000 ms (thick line). B, Same as A with KCNQ1. C, Human I_{Ks} during the AP at fast and slow rates. Some open-state accumulation at fast rate causes a small early jump (arrow), whereas closed-state accumulation in zone 1 creates a reserve that allows the current to increase to a late peak that shortens APD (E). D, HKCNQ1 during the AP at fast and slow rates. Slow kinetics of deactivation cause large open-state accumulation at fast rates and large instantaneous current on depolarization (arrow). Note that in the absence of zone 1 reserve (E), the current stays constant during the AP, lacking the late, repolarizing peak of I_{Ks} (C). E, Human I_{Ks} (black) and KCNQ1 (gray) zone 1 occupancy at CL=250 ms and 1000 ms. Fast-rate accumulation in zone 1 allows I_{Ks} to participate in adaptation. In contrast, little accumulation is seen in zone 1 for KCNQ1. ΔZone 1 is difference in occupancy between CL=250 ms and 1000 ms. F, APD adaptation curves for an AP with

human I_{Ks} (solid line) and KCNQ1 (dashed line). Lack of KCNQ1 accumulation in zone 1 results in less APD shortening at fast rates compared with I_{Ks}.

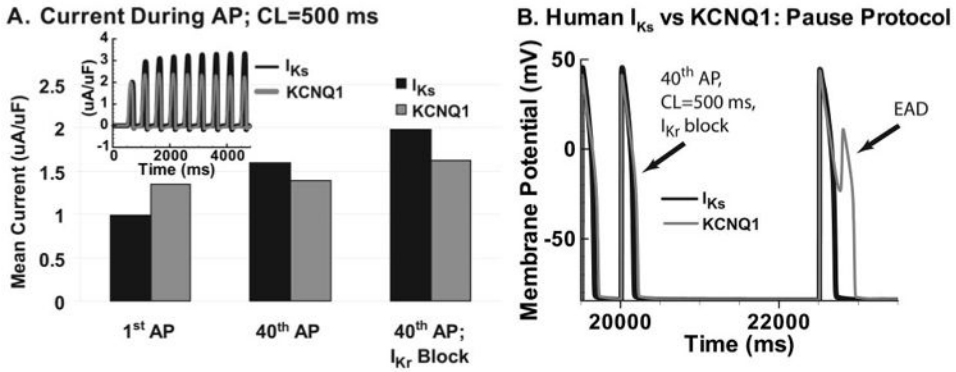

Figure 7.

I_{Ks} participation in RR. A, I_{Ks} accumulation compared with KCNQ1 at CL=500 ms. Mean current during the first AP (left) compared with the 40th AP (middle) shows significant increase for I_{Ks}, whereas KCNQ1 shows only a small increase (time dependence over the first 9 APs is shown in inset). When I_{Kr} is blocked (right), I_{Ks} increases further (doubling compared with first control AP), and KCNQ1 increase is small. B, In presence of I_{Kr} block, pause after 40 APs at CL=500 ms is simulated with I_{Ks} or KCNQ1. Postpause AP with I_{Ks} shows normal repolarization; AP with KCNQ1 develops a pause-induced EAD.